The International Journal of Advanced Manufacturing Technology (2022) 121:5181–5196
https://doi.org/10.1007/s00170-022-09663-6

ORIGINAL ARTICLE

Research on the skiving technology of face gear

Shuai Mo[1,3,4,8,9] · Saisai Wang[2] · Bingrui Luo[2] · Heyun Bao[5] · Guojian Cen[6] · Yunsheng Huang[7]

Received: 6 May 2022 / Accepted: 3 July 2022 / Published online: 14 July 2022

Abstract
Current processing methods of face gear are mainly limited to gear shaping, gear hobbing, and other processes. Gear skiving is a new efficient gear machining technology, in order to realize the high precision and high-efficiency machining of face gear, this paper puts forward the skiving machining technology of face gear. The main research contents include an analysis of the machining principle and model of face gear skiving, deriving the gear skiving tool model by the modified rack according to the meshing principle, and solving the tooth surface model of face gear by envelope method. The findings suggest that the skiving technology can be used in the efficient machining of face gear, which the cutting edge curve of gear skiving tool can be solved by the intersection of rake face and tool tooth face, and the principle error of gear skiving cutter can be effectively reduced after the modification of rack parabola.

Keywords Face gear · Skiving cutter · NURBS surface · Envelope principle

1 Introduction

Face gear transmission is a new type of transmission which is engaged by cylindrical gear and face gear as shown in Fig. 1. It is widely used in aerospace and other fields because of its high bearing capacity and low axial installation sensitivity. Face gear is evolved from cylindrical gear and can transfer the motion of intersecting axis motion. Figure 2b shows the evolution of the different angle parameters of the face gear. The diversity of tooth shapes enables face gears to adapt to a wider range of transmission scenarios.

The machining of face gear is the key research direction of gear; many scholars have carried out a lot of research on the design and machining of face gear [1–11]. Litvin et al. [1] and his team have made a comprehensive research on the generation, machining, and tooth surface contact analysis of face gear; Zschippang et al. [2] deduced the tooth surface equation of face gear according to the envelope of involute gear shaper cutter, and the contact path and undercutting problem of face gear are discussed; Based on the meshing principle, Tang et al. [3] proposed the planing method of machining spur gear with four-axis NC planer and the grinding technology of face gear grinding wheel, and verified the feasibility of the method by using simulation software. He et al. [4] simulated the machining of gear shaping and gear grinding, and found that the meshing performance of grinding wheel is better than that of gear shaping. Wang et al. [5] studied the gear hobbing technology of face gear, proposed a spherical hob based on the basis of traditional hob, and analyzed the principle of evolution from cylindrical hob to spherical hob. Zhou et al. [6] has analyzed the face gear NC milling and tooth surface detection. He proposed a new implicit surface model of face gear and considered the curvature into the tool path planning of face gear machining.

✉ Shuai Mo
moshuai2010@163.com

1 Key Laboratory of Disaster Prevention and Structural Safety of Ministry of Education, Guangxi University, Nanning 530004, China

2 School of Mechanical Engineering, Tiangong University, Tianjin 300387, China

3 State Key Lab of Digital Manufacturing Equipment and Technology, Huazhong University of Science and Technology, Wuhan 430074, China

4 Jiangsu Wanji Transmission Technology Co., Ltd, Taizhou 225400, China

5 National Key Laboratory of Science and Technology On Helicopter Transmission, Nanjing 210016, China

6 Ningbo Zhongda Leader Transmission Equipment Co., Ltd, Ningbo 315301, China

7 Shenzhen Hefa Gear Machinery Co., Ltd, Shenzhen 518000, China

8 School of Mechanical Engineering, Guangxi University, Nanning 530004, China

9 Guangxi Key Laboratory of Disaster Prevention and Engineering Safety, Guangxi University, Nanning 530004, China

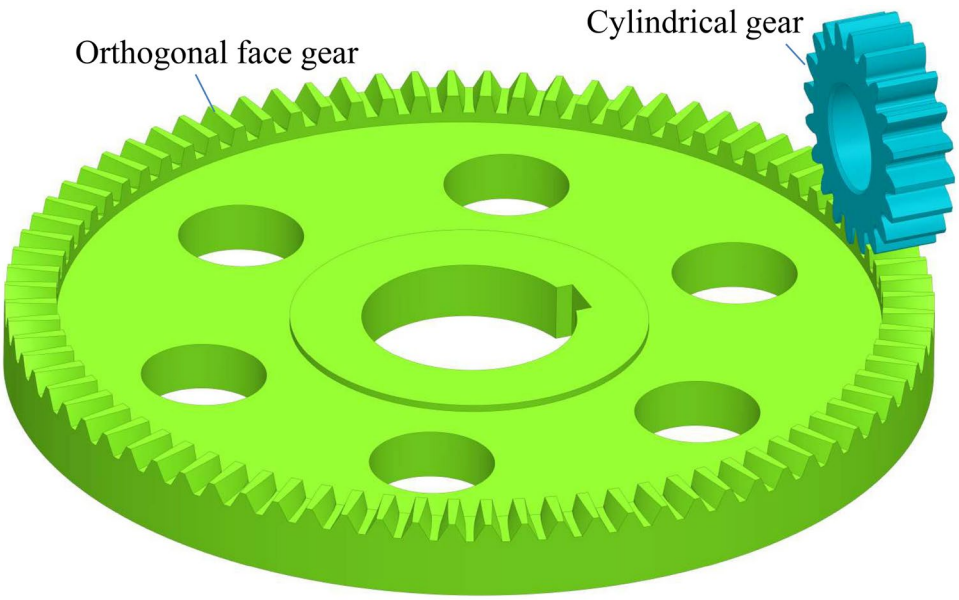

Fig. 1 Schematic diagram of face gear transmission

Mo et al. [7–10] systematically studied the gear design theory and the load distribution uniformity mechanism of the gear transmission system. In order to improve the machining accuracy and efficiency of face gear, seeking a general machining tool with simple structure, high precision, and high efficiency has become an important direction of face gear research.

Gear skiving is a new high-efficiency machining technology that directly cuts the tooth profile from the blank. At present, the research on skiving technology mainly focuses on the machining principle and tool design method [11–20]. Stadtfeld [11] briefly described the skiving machining principle through the evolving relationship between gear and rack and pointed out that the production efficiency of skiving machining is higher than gear hobbing and gear shaping. Tapoglou [12] proposed a new skiving cutting model, which can predict the geometry of non-deformable chips, the shape and size of chips generated in the cutting process, and the characteristics of gear clearance. Based on the surface design theory and manufacturing technology, Li et al. [13, 14] proposed the structural design scheme of cutting tools for involute cylindrical gear and established the mathematical model. Guo et al. [15] studied the calculation method of skiving tooth profile error and analyzed the influence of

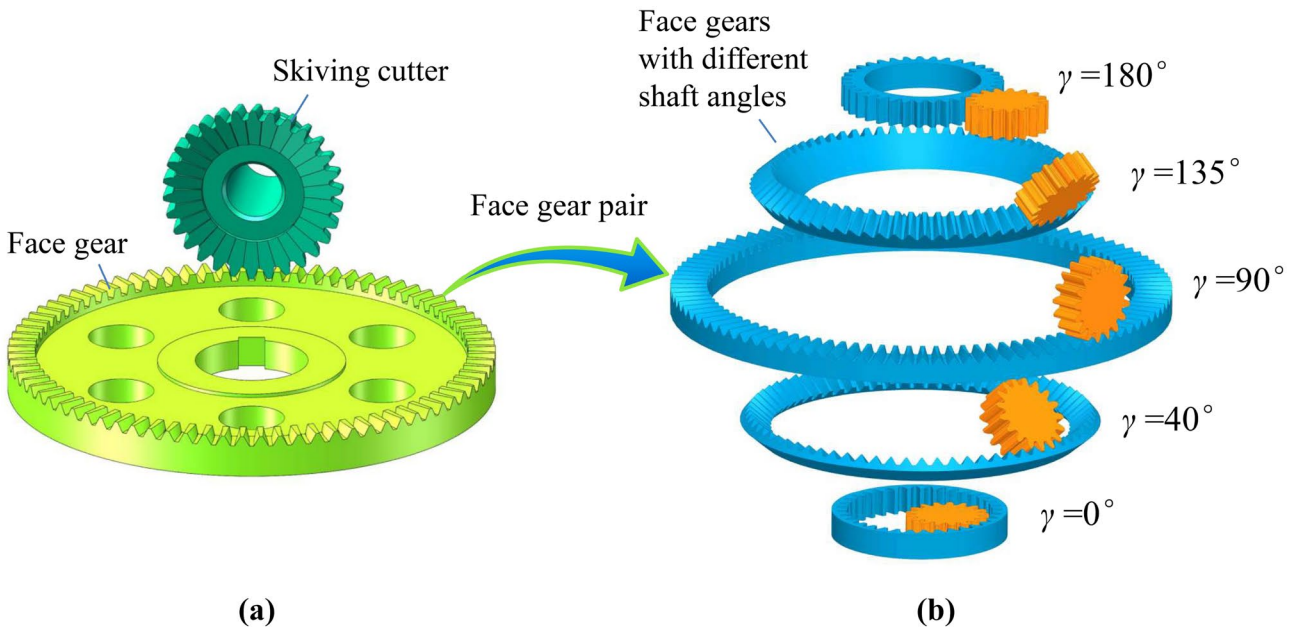

Fig. 2 Face gear and skiving process model: **a** face gear skiving process; **b** evolution of face gears with different shaft angles

skiving tool grinding and rake angle on gear tooth profile error. Based on the principle of generating machining, Jia et al. [16] constructed the skiving motion model, proposed a calculation method of skiving cutting edge tooth profile from the perspective of discrete profile envelope, and solving the model of the machined tooth surface by envelope method. Su et al. [17] deduced the tooth surface of the modified gear skiving cutter from the rack cutter, established the solid model of the new gear skiving cutter, and compared the cutting edge differences established by the reverse envelope method, formula method, modified rack cutter method, and reduced the tooth surface deviation caused by the principle error through modification. Uriu et la. [18] discussed the influence of the shaft intersection angle of internal gear cutting on the tool parameters and tested the common value of shaft angle through cutting simulation and experiment.

At present, the research of skiving machining technology is mostly applied to cylindrical gear, and some achievements have been made in the corresponding tool design and NC machine tool research, but skiving machining technology is rarely used in face gear at present. In order to improve the machining accuracy and efficiency of face gear, this paper puts forward the face gear skiving machining technology as shown on the left side of Fig. 2a, analyzes the face gear skiving machining principle and tool design theory, as well as the content of tool tooth profile error and modification of the skiving cutter, so as to further improve the gear skiving machining technology. In this paper, the machining principle of face gear skiving, tool design and modification are studied in detail. Chapter 1 analyzed the machining principle of face gear skiving. Chapter 2 studied the design method of the face gear skiving cutter. Chapter 3 analyzed the kinematic model of face gear skiving. Chapter 4 analyzed the principle error source of the gear scraping tool and the modification optimization method is proposed.

2 Machining principle of face gear skiving

Gear skiving is an efficient gear processing method, which is similar to gear shaping and has the motion state of gear hobbing at the same time. The skiving movement is shown in Fig. 3, in which the skiving cutter is a helical bevel gear structure, and the helix angle is β, the initial offset distance between the rotation axis of the skiving tool and the center line of the face gear is H, the initial cutting point is P_1, and the final cutting point is P_2, v_s, and v_2 are the linear velocity vector of the skiving tool and the face gear at the initial cutting point, respectively, and v_{s2} is the relative motion speed of the skiving tool along the extension direction of

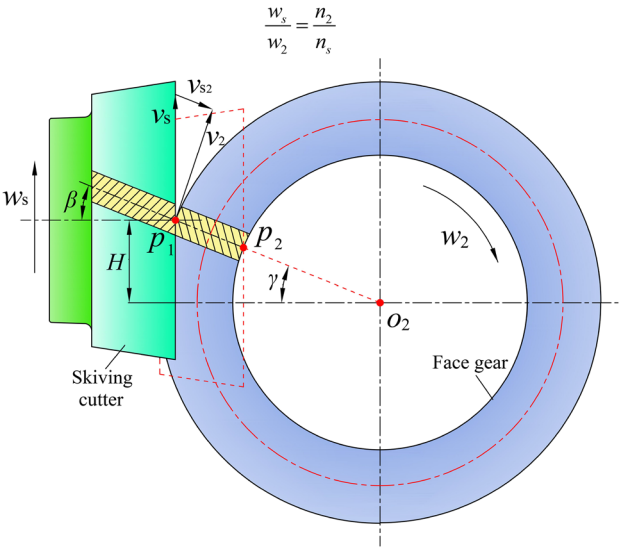

Fig. 3 Schematic diagram of the skiving movement

the tooth profile of the face gear. During machining, the offset distance is continuously adjusted so that the cutting edge of the tool is always tangent to the tooth profile of the face gear at the machining point. The skiving tool and face gear rotate at the angular speed w_s and w_1, and the skiving tool feeds along the face gear tooth direction until the face gear machining is completed. The relationship between the angular velocities w_s and w_1 of the cutter and the face gear is shown in Eq. 1, where n_s and n_2 are the number teeth of the skiving cutter and the face gear, respectively.

$$\frac{w_s}{w_2}=\frac{n_2}{n_s} \tag{1}$$

The skiving machining model is shown in Fig. 4. The tool axis maintains a constant intersection angle γ with the x-axis direction and feeds along the x-axis during machining. The cutter and the face gear make continuous indexing rotation movement and feed along the tooth profile direction of the face gear to be machined. When the tool is in contact with the workpiece, a series of micro gullies are generated due to forced meshing to form the workpiece tooth surface. Under the linkage of the machine tool, the tooth skiving tool advances along the workpiece tooth profile direction, and then makes feeding movement along the y-axis direction to remove the materials corresponding to the target profile layer by layer, finally complete the processing of the gear tooth profile.

The gear skiving process is shown in Fig. 5. The position of the tool relative to the workpiece is 1–2-3–4-5 in turn. The cutting starts from the tooth root of the cutting

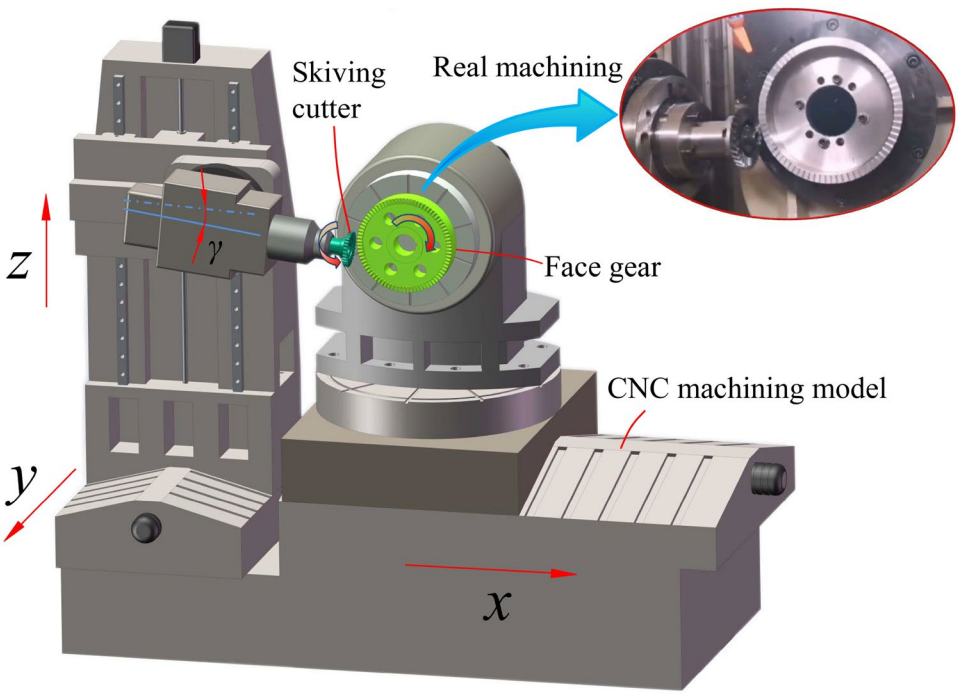

Fig. 4 Schematic diagram of gear skiving machine tool

edge and moves towards the top of the face gear as the cutting proceeds, as shown in position 2. The cutting point starts the processing of the tooth root at position 3. After the tooth root processing is completed, the gear skiving tool exits the meshing, and the tooth profile of the face gear is gradually formed under the forced meshing and cutting movement of the gear skiving [11].

3 Design of the skiving cutter

3.1 Tooth surface of gear skiving cutter

The structure of the gear skiving cutter is helical bevel gear. This paper deduces the tooth surface of the modified gear skiving cutter from the rack cutter. Figure 6 is a schematic diagram

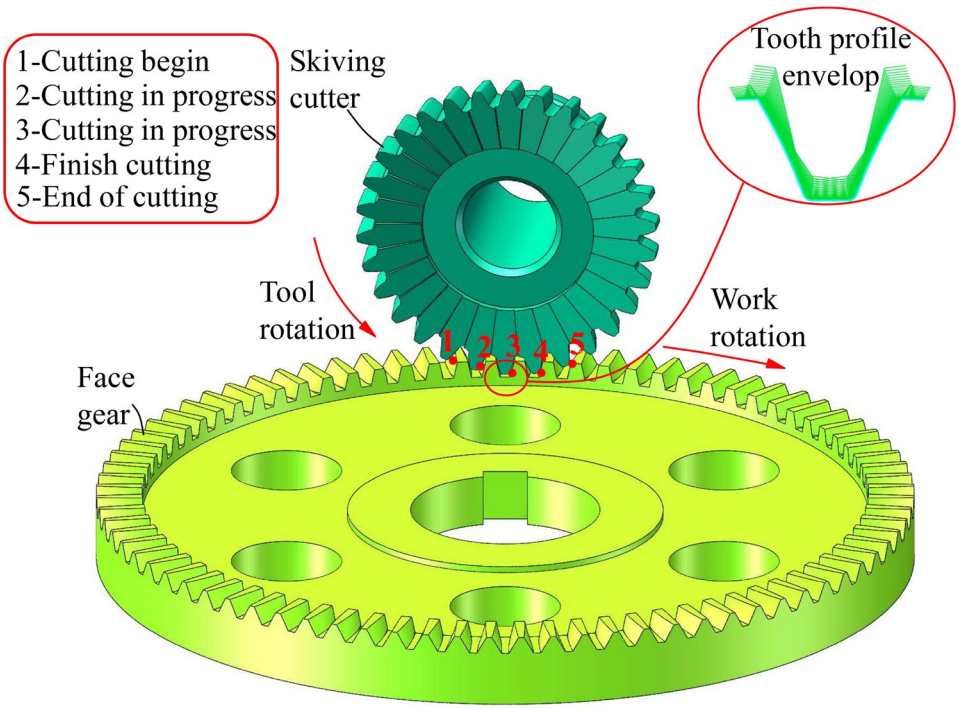

Fig. 5 Schematic diagram of skiving process

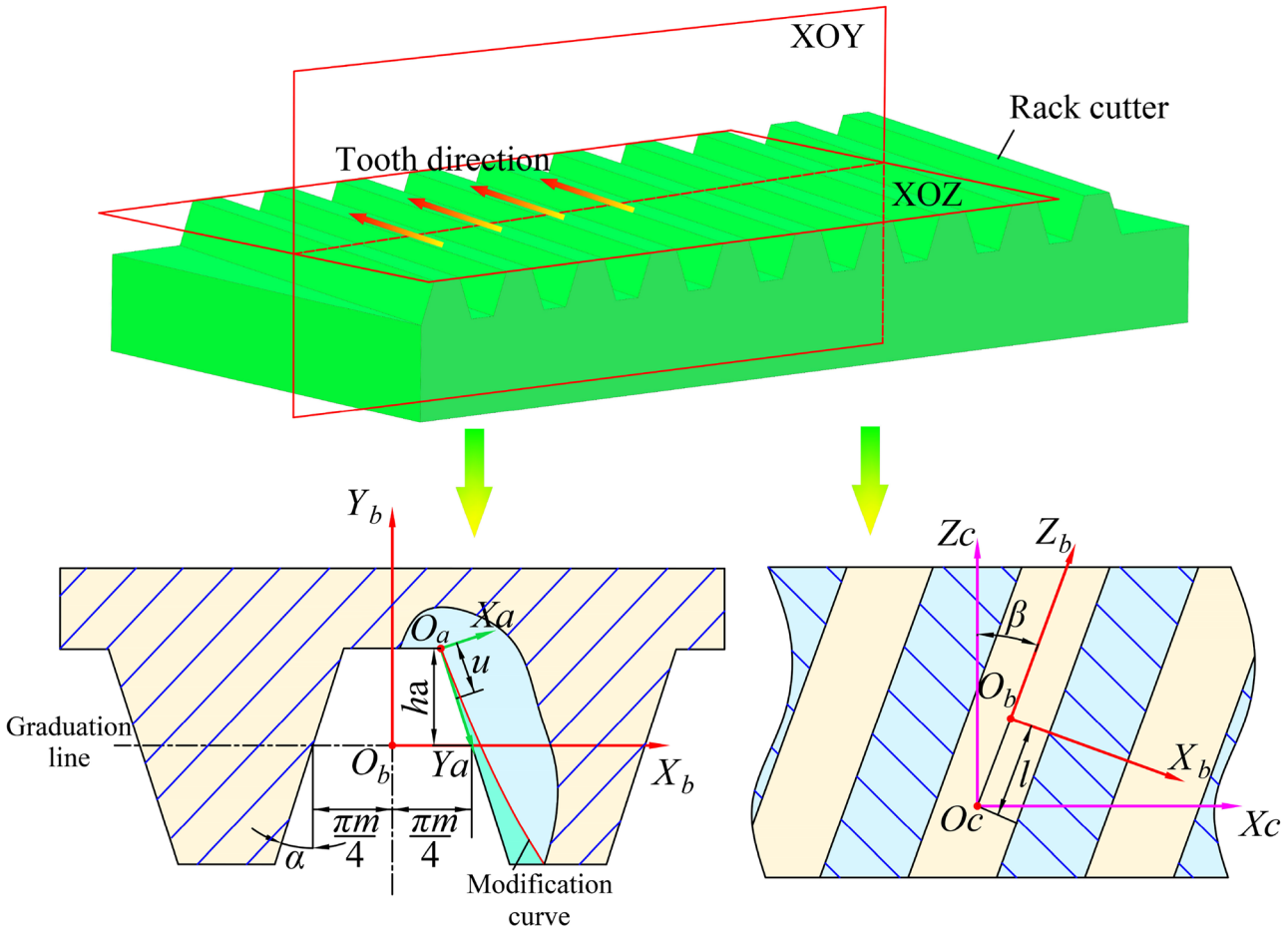

Fig. 6 Tooth profile diagram of modified rack cutter

of the tooth profile of the rack cutter, according to the tooth profile error of the gear skiving cutter gradually increases from the top to the root of the tooth, and the starting point of the modification curve is set at the root of the rack. In the coordinate system S_a, the rack tool tooth profile can be expressed as $r_a = [au^2\ u\ l\ 0]^T$, where a is the parabola modification coefficient, u is the distance from the cutting point to the origin O_a, and l is the rack cutter tooth direction position parameter. The tooth profile equation and the normal vector of the rack cutter are expressed as Eq. 7 in the coordinate system S_c [17].

$$r_c(u,l) = M_{c,b} \cdot M_{b,a} \cdot r_a(u,l) \tag{2}$$

$$n_c(u,l) = \frac{\partial r_c(u,l)}{\partial u} \cdot \frac{\partial r_c(u,l)}{\partial l} \tag{3}$$

$$M_{c,b} = \begin{bmatrix} \cos\beta & \sin\beta & 0 & 0 \\ -\sin\beta & \cos\beta & 0 & 0 \\ 0 & 0 & 1 & l \\ 0 & 0 & 0 & 1 \end{bmatrix} \tag{4}$$

$$M_{b,a} = \begin{bmatrix} \cos\alpha & \sin\alpha & 0 & \frac{-\pi\cdot m}{4} + h_a \cdot \sin\alpha \\ -\sin\alpha & \cos\alpha & 0 & \frac{h_a}{\cos\alpha} \\ 0 & 0 & 1 & 0 \\ 0 & 0 & 0 & 1 \end{bmatrix} \tag{5}$$

where M_{ba} is the transformation matrix from coordinate system, S_a to coordinate system, S_b, and M_{cb} is the transformation matrix from coordinate system, S_b to coordinate system S_c, and ha is the addendum height.

Figure 7 shows the coordinate system of the rack cutter for machining the continuously modified gear skiving cutter, S_c is the rack cutter reference coordinate system. S_{s0} is the gear skiving cutter reference coordinate system, S_s is the gear skiving cutter moving coordinate system, and $l{\cdot}\tan\alpha_0$ is the displacement at different tooth direction positions of rack cutter. According to the involute gear generating principle, the corresponding rack moves $r_a{\cdot}\varphi$ along the pitch line. The meshing condition of the gear skiving cutter and the rack cutter is that the connecting line between any point on the cutting edge of the rack cutter and the instantaneous center I is the normal

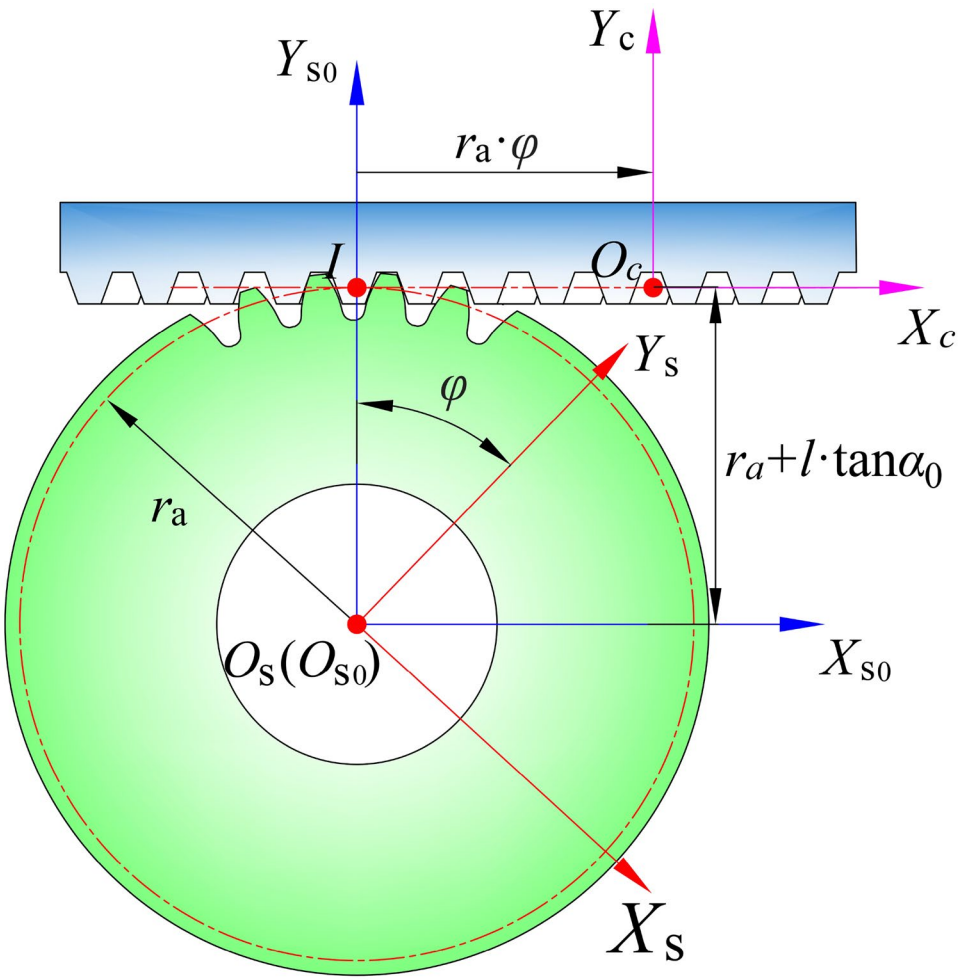

Fig. 7 Coordinate system of gear skiving tool for rack cutter machining

direction of the cutting point, that is, the angle of rotation φ satisfy the Eq. 6. The tooth surface position vector r_s and normal loss n_s of the skiving cutter in S_2 are

$$\varphi = [(l \cdot \tan\alpha_0 + y_c) \cdot \frac{n_{cx}}{n_{cy}} - x_c]/r_a \tag{6}$$

$$\begin{cases} r_s(u,l) = M_{s,s0} \cdot M_{s0,c} \cdot r_c(u,l) \\ n_s(u,l) = M_{s,s0} \cdot M_{s0,c} \cdot n_c(u,l) \end{cases} \tag{7}$$

$$M_{s,s0} = \begin{bmatrix} \cos\varphi & -\sin\varphi & 0 & 0 \\ \sin\varphi & \cos\varphi & 0 & 0 \\ 0 & 0 & 1 & 0 \\ 0 & 0 & 0 & 1 \end{bmatrix} \tag{8}$$

$$M_{s0,c} = \begin{bmatrix} -1 & 0 & 0 & -r_a \cdot \varphi \\ 0 & -1 & 0 & -l \cdot \tan\alpha_0 - r_a \\ 0 & 0 & 1 & 0 \\ 0 & 0 & 0 & 1 \end{bmatrix} \tag{9}$$

where $M_{s,s0}$ are the transformation matrix from coordinate system, S_{s0} to coordinate system S_s, $M_{s0,c}$ are the transformation matrix from the coordinate system, S_c to the coordinate system S_{s0}, r_a is the radius of the workpiece pitch circle, and φ is the rotation angle of the gear skiving tool.

Non-uniform rational B-splines (NURBS) surface is the tensor product form of the corresponding curve and has good local precision. It is a very excellent modeling method. For B-spline surface fitting of the surface type value points, the control vertices in a topological rectangular array should be inversely calculated. Generally, the inverse calculation problem of the surface is resolved into a two-stage curve inverse calculation. Fitting the tooth surface of the skiving tool, and selecting $K \times L$ type value points, set the value points in parameter u direction as $F_{i,j}$.

$$\begin{bmatrix} 5 & 1 & & & & & \\ 1 & 4 & 1 & & & & \\ & 1 & 4 & 1 & & & \\ & \vdots & \vdots & \vdots & & & \\ & & 1 & 4 & 1 & & \\ & & & 1 & 4 & 1 & \\ & & & & & 1 & 5 \end{bmatrix} \begin{bmatrix} V_{2,j} \\ V_{3,j} \\ V_{4,j} \\ \vdots \\ V_{m-3,j} \\ V_{m-2,j} \\ V_{m-1,j} \end{bmatrix} = 6 \begin{bmatrix} F_{1,j} \\ F_{2,j} \\ F_{3,j} \\ \vdots \\ F_{m-4,j} \\ F_{m-3,j} \\ F_{m-2,j} \end{bmatrix} \tag{10}$$

$$\begin{cases} V_{1,j} = V_{2,j} \\ V_{m,j} = V_{m-1,j} \end{cases} \tag{11}$$

According to the free endpoint condition (10), the u-direction control points $V_{i,j}$ can be obtained, taking the control points $V_{i,j}$ as the shape point in the w direction, the B-spline surface control point $p_{i,j}$ is obtained in the same way. Equation (12) is the NURBS surface fitting equation, where $N_{i,3}(u)$ and $N_{j,3}(w)$ are the basis functions.

$$\begin{cases} P(u,w) = \sum_{i=0}^{K-1} \sum_{j=0}^{L-1} p_{i,j} N_{i,3}(u) N_{j,3}(w) \\ 0 \le u \le 1, 0 \le w \le 1 \end{cases} \tag{12}$$

3.2 Cutting edge solution

3.2.1 Rake face model

In the process of gear skiving, there is an axial intersection angle between the tool and the workpiece. Therefore, the plane inclined to a certain angle with the end face is used as the rake face to make the cutting angles of the two edges of the gear skiving cutter close and reduce the edge error of the gear to be processed. In Fig. 8, the coordinate system S_s-Oxyz is the rake face coordinate system, S_a-O$_a x_a y_a z_a$ is the auxiliary face coordinate system, and S_1-O$_1 x_1 y_1 z_1$ is the tool motion coordinate system.

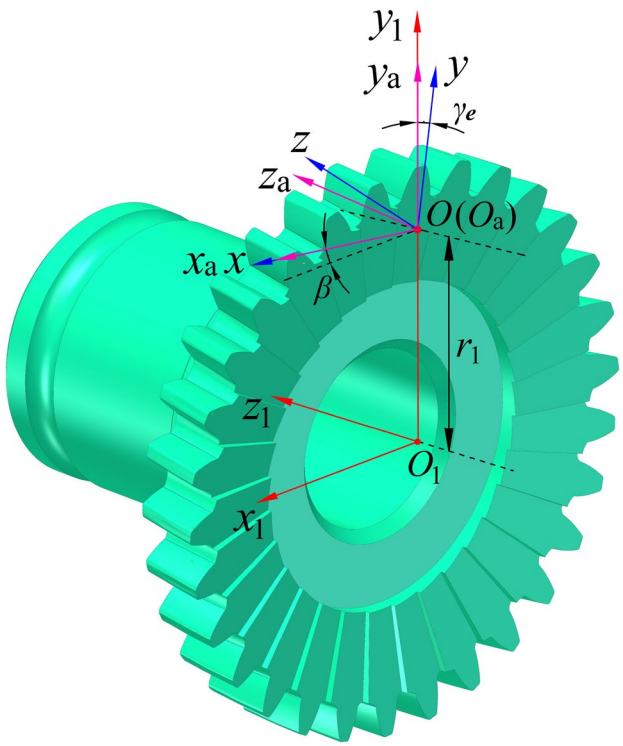

Fig. 8 Rake face coordinate system

The rake face normal vector can be expressed as $n(0,0,1)$ in the coordinate system S, according to Eq. (13), the normal vector of the rake face is $n_1(\cos\gamma_e \sin\beta, -\sin\gamma_e, \cos\gamma_e \cos\beta)$ [13, 14].

$$n_1^T = B_2 B_1 n^T \tag{13}$$

$$M_{a,s} = \begin{bmatrix} 1 & 0 & 0 & 0 \\ 0 & \cos\gamma_e & \sin\gamma_e & 0 \\ 0 & \sin\gamma_e & \cos\gamma_e & 0 \\ 0 & 0 & 0 & 1 \end{bmatrix} \tag{14}$$

$$M_{1,a} = \begin{bmatrix} \cos\beta & 0 & \sin\beta & 0 \\ 0 & 1 & 0 & r_1 \\ \sin\beta & 0 & \cos\beta & 0 \\ 0 & 0 & 0 & 1 \end{bmatrix} \tag{15}$$

where γ_e is the rake angle of the tool, β is the tool helix angle, $M_{a,s}$ is the matrix of the transformation from the rake surface coordinate system, S_s to the auxiliary surface coordinate system S_a, $M_{1,a}$ is the matrix of the transformation from the auxiliary surface coordinate system, S_a to the tool motion coordinate system S_1, and the rake surface equation in S_1 is:

$$x_1 \cos\gamma_e \sin\beta - (y_1 - r_1)\sin\gamma_e + z_1 \cos\gamma_e \cos\beta = 0 \tag{16}$$

3.2.2 Solution of cutting edge intersection

The solution of the skiving cutting edge curve based on the conjugate principle is equivalent to the solution of the intersection of two curved surfaces. The envelope surface of the rack tool tooth surface is the conjugate surface of the skiving tool. The component of the conjugate surface fitting point in the coordinates can be expressed as $x_2 = P_1(u,w)$, $y_2 = P_2(u,w)$, and $z_2 = P_3(u,w)$. The rake surface equation can be written as $f(x_2,y_2,z_2) = 0$, in this paper, the Newton iteration method is used to approximate the distance between the vertex of conjugate surface mesh and rake face to obtain the main cutting edge. Bring the four vertices of the conjugate face-fit point cloud mesh element into the rake face equation, and the corresponding function values are $p(u_i,w_j)$, $p(u_i,w_{j+1})$, $p(u_{i+1},w_j)$, and $p(u_{i+1},w_{j+1})$. The main calculation steps of the main cutting edge are as follows (Fig. 9):

(a) Bring the components $x_2 = P_1(u,w)$, $y_2 = P_2(u,w)$, and $z_2 = P_3(u,w)$ of the vertices of the mesh in the fitting point cloud into $f(x_2,y_2,z_2)$ and judge the symbol of the vertices of each mesh (greater than 0 is recorded as "+", otherwise it is recorded as "−").

(b) Judge the calculation results of (a). If the symbols of the calculation results of the four vertices in the grid are the same, the grid unit has no intersection with the equal rake face, otherwise, go to (c).

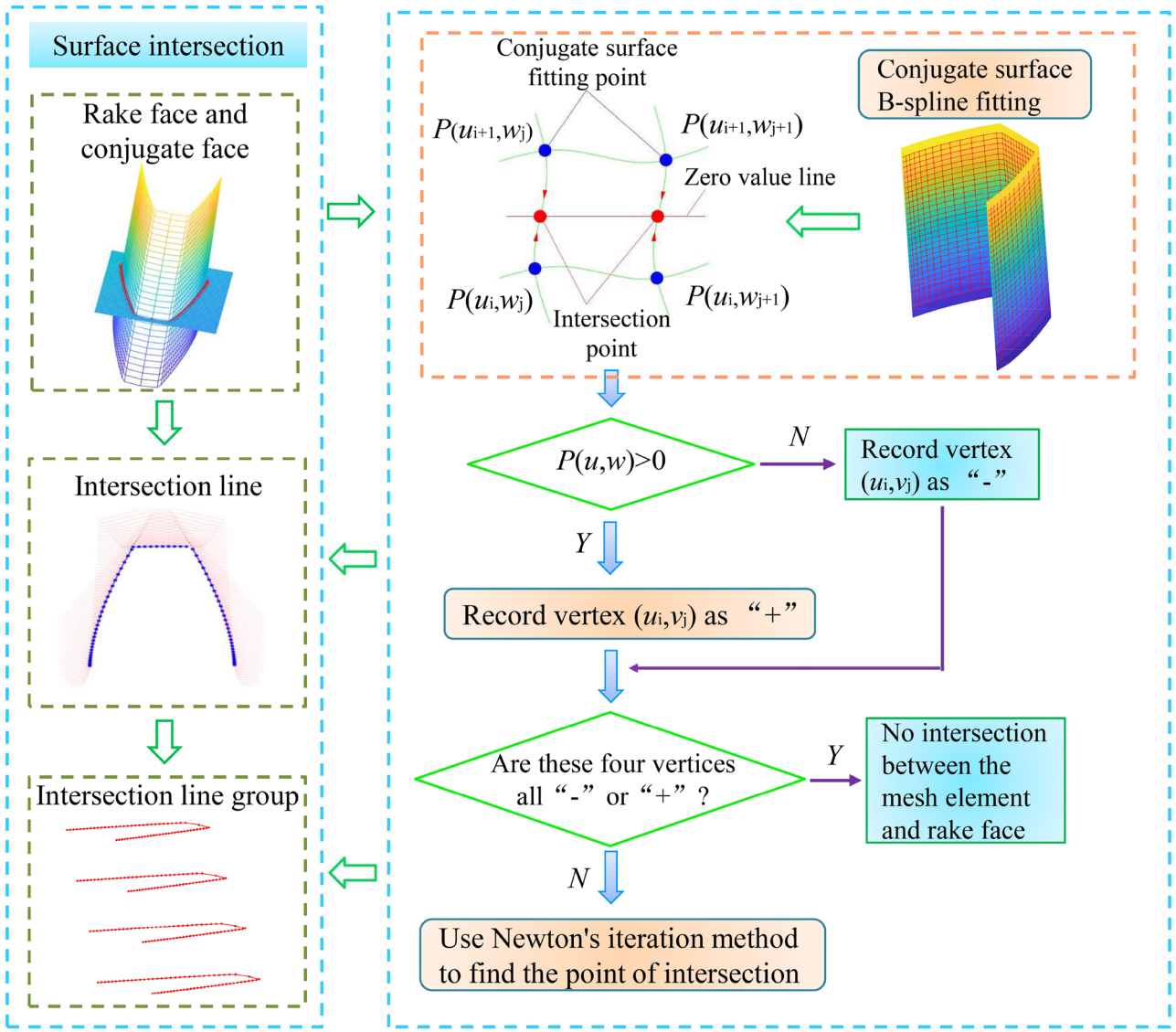

Fig. 9 Schematic diagram of surface intersection

(c) For the element edges with different signs at both ends, the Newton iteration method can be used to calculate the intersection point. Let $h(u_{i+1},w_{j+1})$ be "−", $h(u_{i+1},w_j)$ be "+", and $u_t = u_{i+1}$ in the intersection point (u_t,w_t), and w_t can be calculated by Newton iteration formula (17).

$$w_{k+1} = w_k - \frac{w_k - w_{k-1}}{h(u_t,w_k) - h(u_t,w_{k-1})} h(u_t,w_k) \tag{17}$$

Let $w_1 = w_j$ and $w_2 = w_{j+1}$ to set the iteration accuracy $\xi = 0.0001$, $w_t = w_{k+1}$ when Eq. (17) iteration to $w_{k+1} - w_k < \xi$, calculate the corresponding u and w values and substitute them into Eq. (16) to obtain the intersection point (Table 1). Figure 10 is the schematic diagram of solving the cutting edge curve when the rake face intersects with the tool tooth surface. The cutting edge curve in the figure is the intersection line between the rake face and the tool tooth surface, the envelope curve is the intersection line between the rake face and the rack tool envelope surface, r_a is the addendum circle, r_b is the dividing circle, and r_f is the root circle.

3.3 Skiving cutter model

Taking the orthogonal face gear as an example, build the three-dimensional model of a gear skiving cutter. The design flow is shown in Fig. 11, the rake face equation is

Table 1 Intersection coordinates mm

Point	*x*	*y*	*z*
1	−2.0160	−42.4947	6.6389
2	−1.9979	−42.5991	6.6215
3	−1.9783	−42.7081	6.6033
4	−1.9569	−42.8214	6.5843
5	−1.9337	−42.9390	6.5643
6	−1.9087	−43.0609	6.5435
7	−1.8817	−43.1869	6.5218
8	−1.8527	−43.3171	6.4993
9	−1.8216	−43.4514	6.4759
…	…	…	…
…	…	…	…
494	3.4700 16.774	−42.6117	5.8513
495	3.4806	−42.5077	5.8646

obtained with reference to Sect. 3.2; modulus $m = 3$ mm, the number of teeth $z_2 = 80$, shaft angle $\gamma = 8°$. Calculate the point cloud of the tooth surface of the conjugate surface and fit it with the cubic B-spline surface. The cutting edge is obtained by fitting the intersection with Eq. (18):

$$\begin{cases} k(u') = \sum_{j=0}^{n} d_j N_{j,3}(u') \\ 0 \le u' \le 1 \end{cases} \tag{18}$$

Imported the cutting edge point cloud fitted by the cubic B-spline curve into CAD software to construct the tooth surface of gear skiving cutter, the single tooth model is constructed by surface stitching, and the solid model of gear turning tool is obtained by single tooth solid array.

4 Kinematic model of the face gear skiving

4.1 Gear skiving coordinate system

Figure 12 is the gear skiving coordinate system established according to the tooth surface generation principle [1–4], in which S_s-$O_s x_s y_s z_s$ is the tool motion coordinate system, S_2-$O_2 x_2 y_2 z_2$ is the surface gear motion coordinate system, S_{s0}-$O_{s0} x_{s0} y_{s0} z_{s0}$ is the tool reference coordinate system, and S_{20}-$O_{20} x_{20} y_{20} z_{20}$ is the surface gear reference coordinate system. φ_2 is the rotation angle of the face gear, φ_s is the rotation angle of the skiving cutter, r is the distance between the center point of the face gear and the center point of the skiving cutter, and γ is the axis intersection angle. The envelope equation of face gear skiving tooth surface is as follows:

$$\begin{cases} r_2(u, l) = M_{2,s} \cdot r_s(u, l) \\ M_{2,s} = M_{2,20} \cdot M_{20,s0} \cdot M_{s0,s} \end{cases} \tag{19}$$

$$M_{20,s0} = \begin{bmatrix} 0 & 0 & -1 & -r \cdot \cos\gamma \\ 0 & 1 & 0 & r \cdot \sin\gamma \\ 1 & 0 & 1 & 0 \\ 0 & 0 & 0 & 1 \end{bmatrix} \tag{20}$$

$$M_{s0,s} = \begin{bmatrix} \cos\varphi_s & \sin\varphi_s & 0 & 0 \\ -\sin\varphi_s & \cos\varphi_s & 0 & 0 \\ 0 & 0 & 1 & 0 \\ 0 & 0 & 0 & 1 \end{bmatrix} \tag{21}$$

$$M_{2,20} = \begin{bmatrix} \cos\varphi_2 & -\sin\varphi_2 & 0 & 0 \\ \sin\varphi_2 & \cos\varphi_2 & 0 & 0 \\ 0 & 0 & 1 & 0 \\ 0 & 0 & 0 & 1 \end{bmatrix} \tag{22}$$

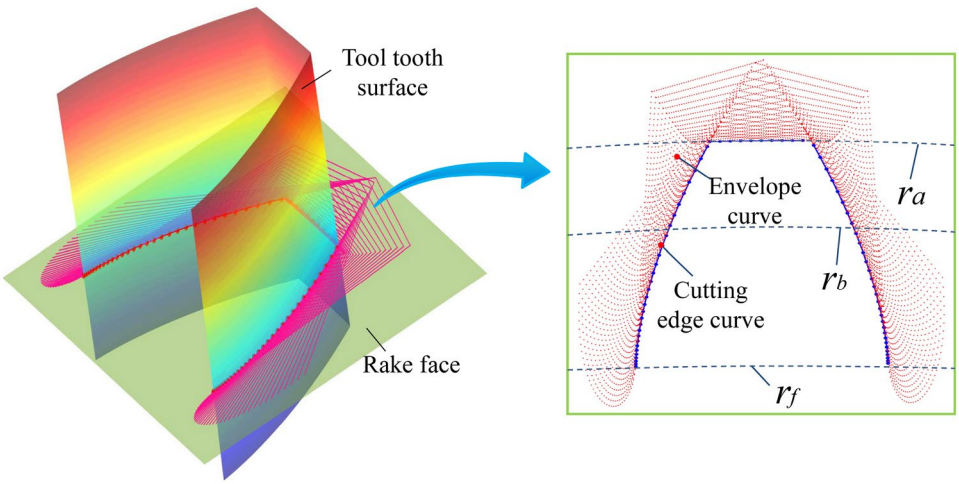

Fig. 10 Schematic diagram of cutting edge envelope solution

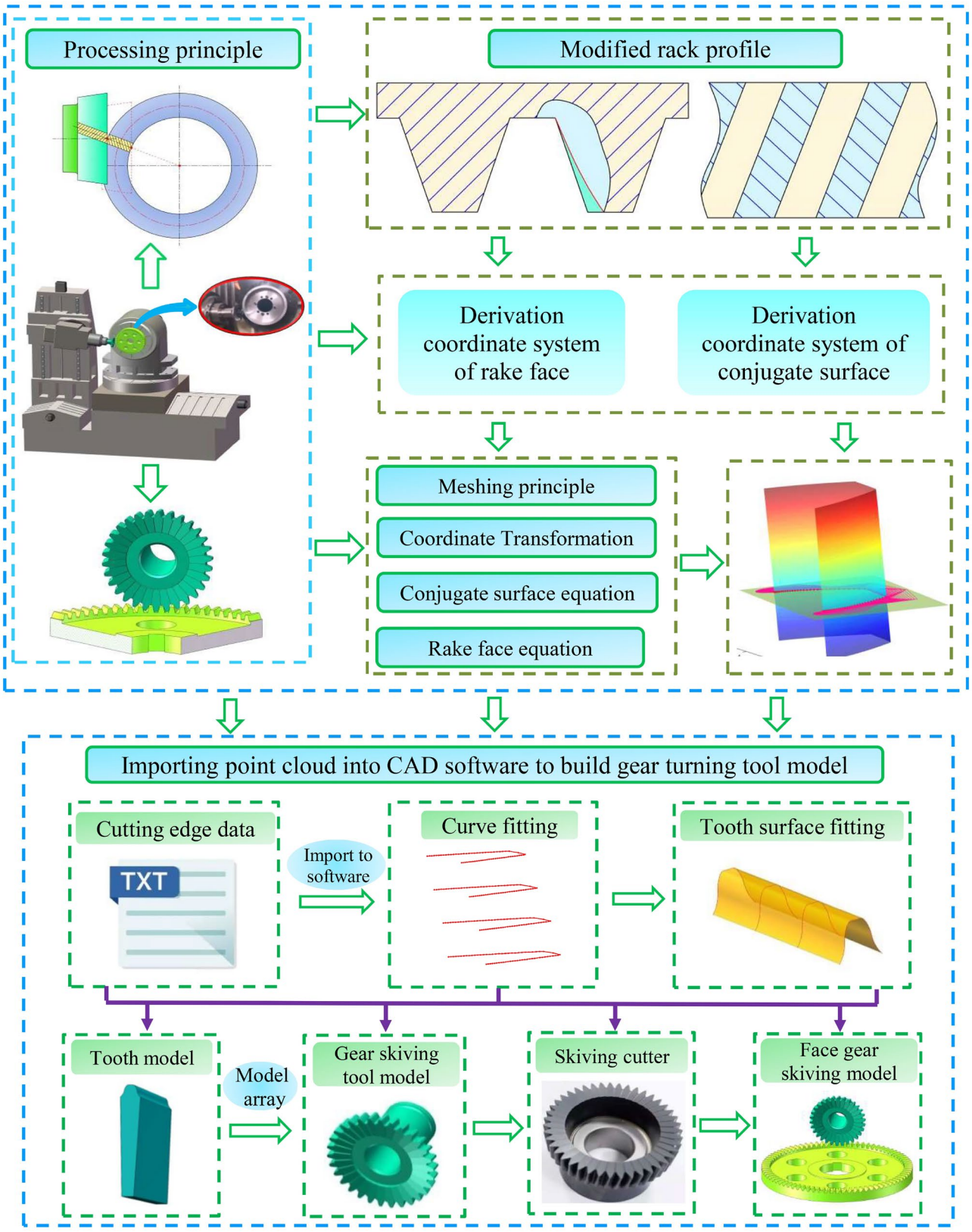

Fig. 11 Gear turning tool design process

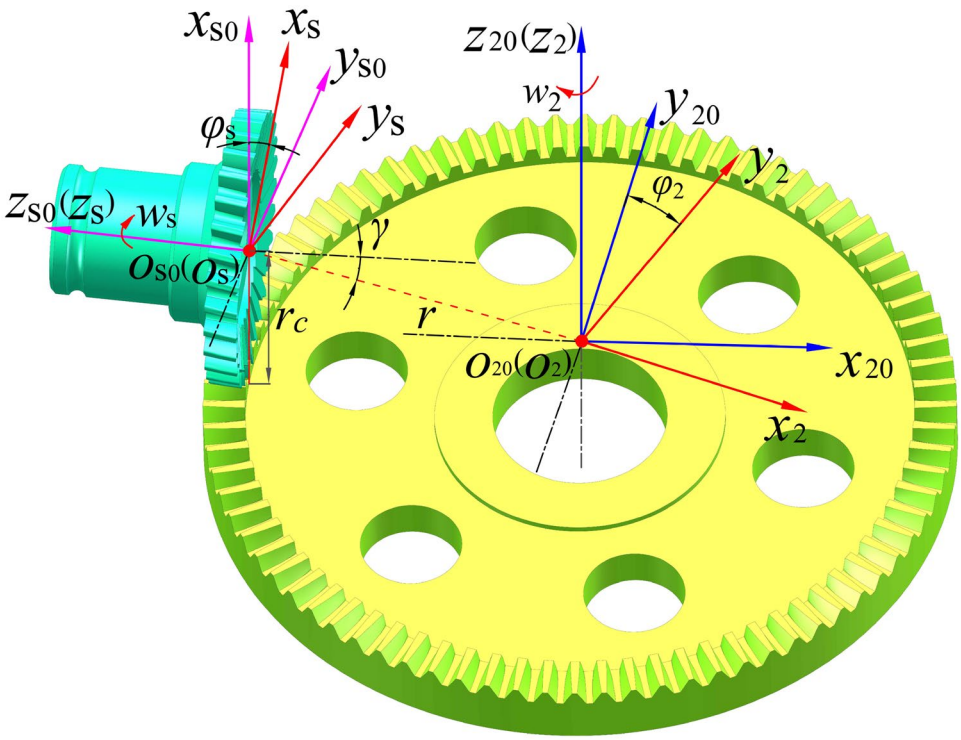

Fig. 12 Gear skiving coordinate system

where M_{s0} are the coordinate conversion matrix from S_s to S_{s0}, $M_{20,s0}$ are the coordinate conversion matrix from S_{s0} to S_{20}, and $M_{2,20}$ are the coordinate conversion matrix from S_{20} to S_2.

4.2 Solution of enveloping surface model of face gear

The machining process of face gear can be seen as the conjugate evolution movement of the skiving cutter and face gear. The envelope of the gear skiving tool's cutting edge is the tooth surface of face gear. Figure 13 shows the projection of the cutting edge point cloud in the tooth direction. Take O as the center, set z_r uniform radii within the range $[r_a,r_f]$, all cutting edge point clouds are divided into regions in the circles corresponding to these radii. Because the tooth surface of face gear is located outside the point cloud space of the cutting edge in the process of machining movement, the outer envelope curve of the cutting edge is the envelope curve of face gear. Therefore, in the i-th ring determined by radius $[z_i,z_i+\Delta z]$, the two points P_1 and P_2 furthest from the z-axis in the envelope point cloud of all cutting edges are the points of the face gear envelope at the radius z_i. Thus, the envelope of face gear can be solved by identifying P_1 and P_2 points corresponding to all Z_r radii [15, 16].

According to the working principle of skiving, changing the rotation angle φ_s of the skiving tool and the tooth feed amount r in the coordinate system shown in Fig. 6, constitute cutting edge point cloud for different feeds to extract the continuous tooth surface enveloping line, and finally constitutes the enveloping tooth surface of the face

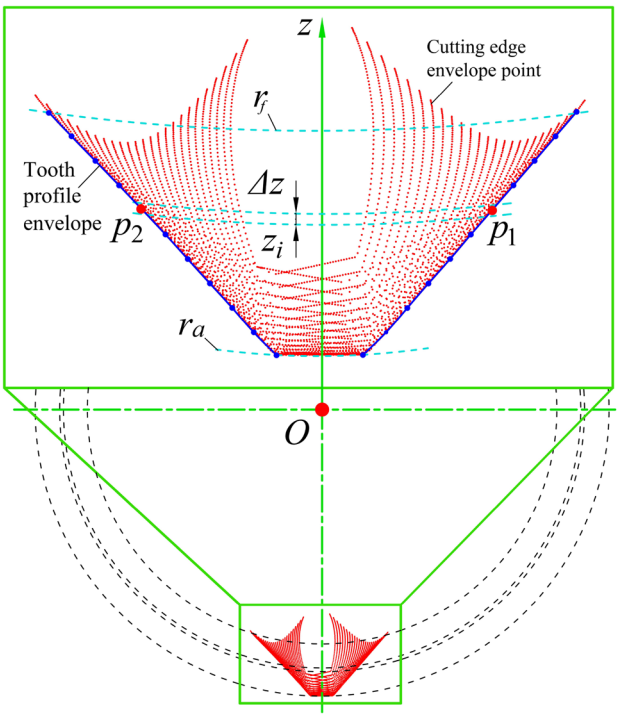

Fig. 13 Cutting edge track tooth direction section

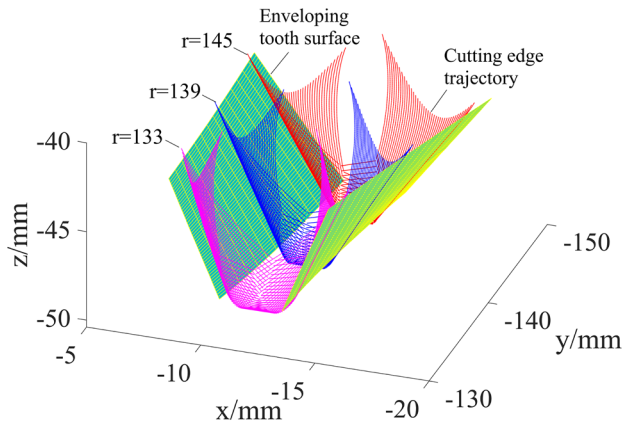

Fig. 14 Schematic diagram of enveloping cutting edge

gear as shown in Fig. 14. In order to improve the accuracy of tooth surface extraction of face gear, the extracted point cloud is fitted with NURBS surface, and Eq. (23) is the surface fitting equation.

$$\begin{cases} P(u,w) = \sum_{i=0}^{M-1}\sum_{j=0}^{L-1} p_{ij}N_{i,3}(u)N_{j,3}(w) \\ 0 \le u \le 1, 0 \le w \le 1 \end{cases} \tag{23}$$

5 Error analysis and modification of gear skiving

5.1 Error analysis

The tooth surface of the tool after grinding can be regarded as composed of the intersection line of the rake surface and a series of modified tooth surfaces, the processed gear is formed through the development processing of the tool, and the cutting motion track of the tool cutting edge has meshed with the processed gear. Therefore, there is no error only when the projection of the cutting edge on the end face coincides with the theoretical tooth shape [20, 21]. However, due to the existence of front angle and back angle, the projection of the cutting edge on the end face is not an involute, so the principle error of gear skiving cutter is formed, as shown in Fig. 15. Where α_e and γ_e are the back angles and front angles, respectively, r_a is the radius of the addendum circle, r_b is the radius of the dividing circle, and r_f is the radius of the root circle.

Table 2 Scraping machining parameters

Parameter	Skiving cutter	Face gear
Pressure angle/°	20	20
Modulus/mm	3	3
Number of teeth	31	90
Helix angle/°	5	-
Back edge angle/°	5	-

Table 2 shows the specific parameters of gear skiving. Solving the point cloud of the cutting edge corresponding to different front and back angles and analyzing the error according to the content of Sect. 3.2. Figure 16 shows the tooth profile deviation corresponding to different front angles. It can be seen from the figure that the tooth profile error gradually increases from the tooth top to the tooth root, and increases with the value of the tool rake angle. When the back angle $\alpha_e = 6°$ and the front angle $\gamma_e = 5°$, the maximum error value of the left tooth profile is about 24 μm and the maximum error value of the right tooth profile is about 20 μm. The errors on both sides of the tooth profile are different, this is due to the asymmetric projection of the tooth profiles on both sides of the front face.

5.2 Tool profile modification

Figure 17 shows the variation trend of tooth profile deviation on the right side of the gear skiving cutter under different

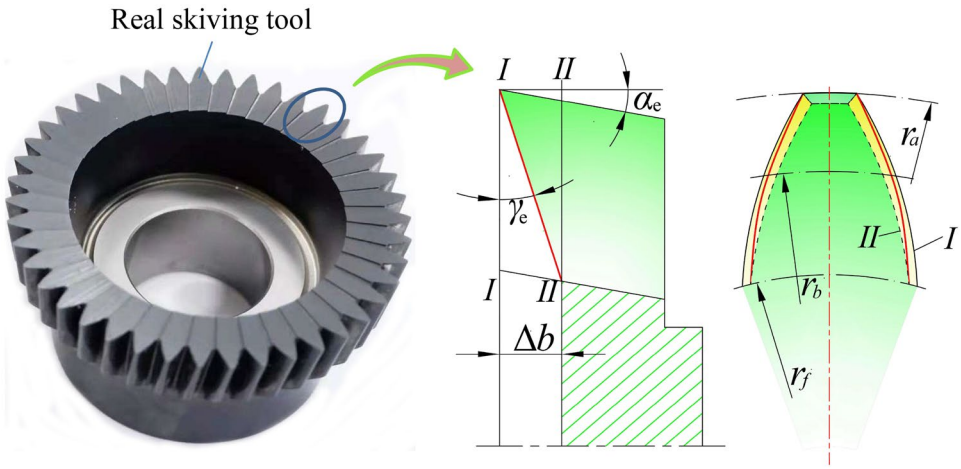

Fig. 15 Schematic diagram of cutting edge error

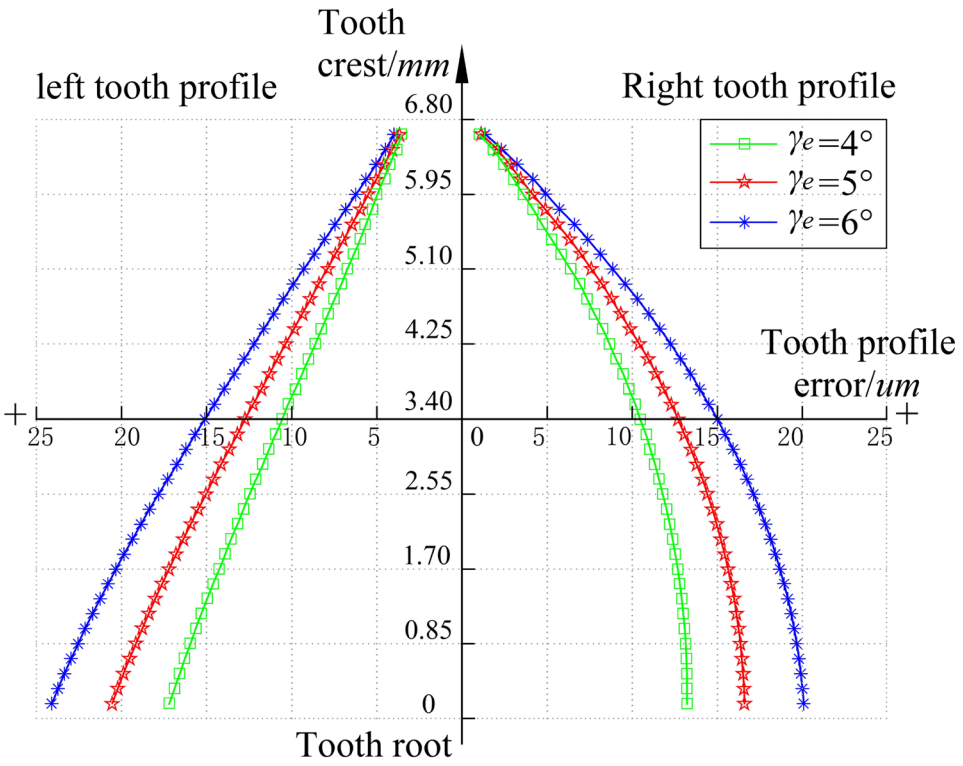

Fig. 16 Tooth profile error on both sides of the tool

modification coefficients. Compared with the unmodified tooth profile deviation curve, with the increase of the modification coefficient, the tooth profile deviation first increases, then decreases, and finally increases. When the modification coefficient is $a=0.0005$, the overall tooth profile deviation is the smallest. Figure 18 shows the variation trend of the left tooth profile deviation of the gear skiving cutter under different modification coefficients. Similar to the variation trend of the right tooth profile deviation, the tooth profile deviation increases first, then decreases, and finally increases. When the modification coefficient $a=0.0004$, the overall tooth profile deviation is the smallest.

5.3 Influence of the skiving cutter error on tooth surface

Let the rake angle $\alpha_e=0°$ and the front angle $\gamma_e=0°$, and take the obtained tooth surface as the error-free reference

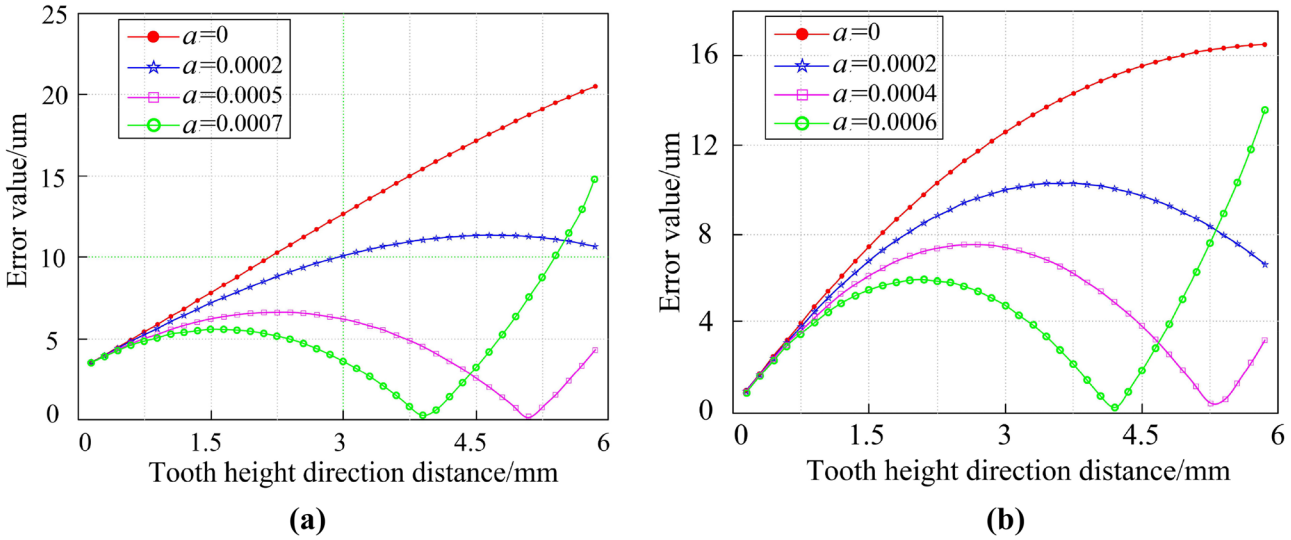

Fig. 17 Tooth profile error: **a** left tooth profile error; **b** right tooth profile error

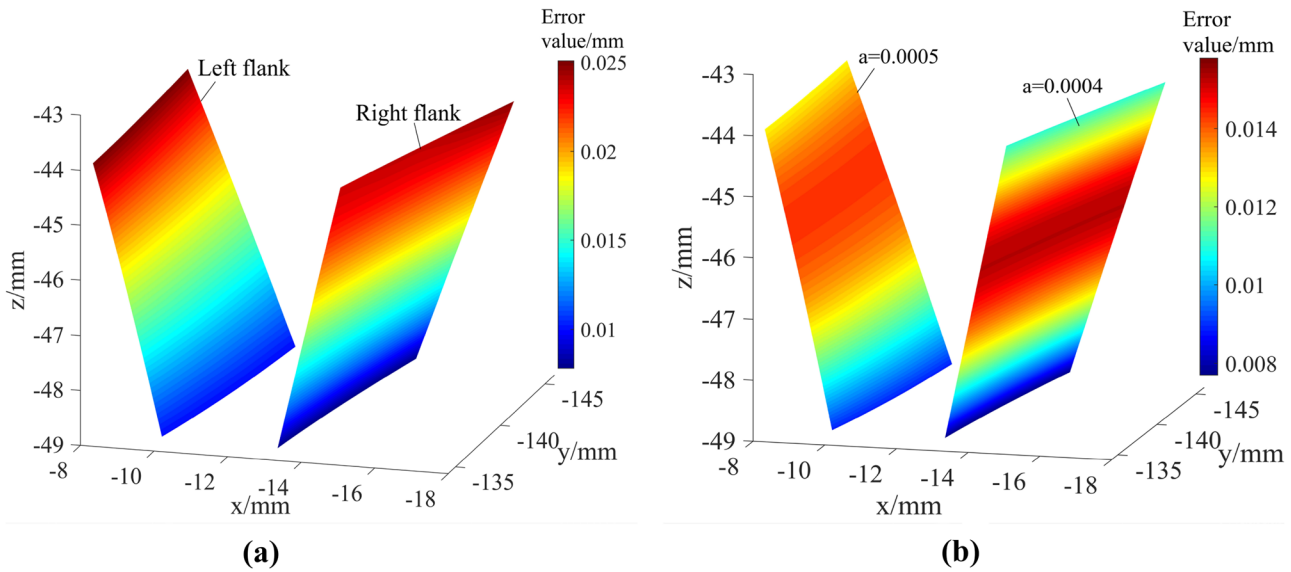

Fig. 18 Tooth surface error: **a** tooth surface error without modification; **b** modified tooth surface error

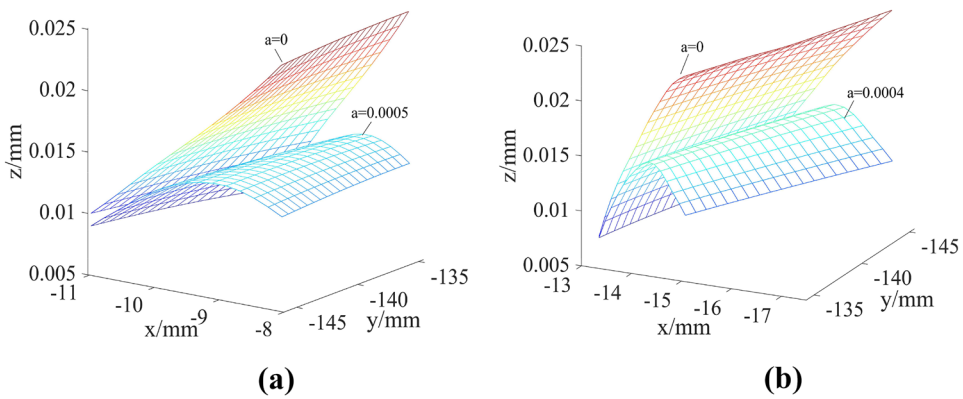

Fig. 19 Error diagram of face gear tooth surface: **a** error diagram of left tooth surface; **b** error diagram of right tooth surface

tooth surface. Take the front angle $\alpha_e = 5°$ front angle $\gamma_e = 5°$ enveloping tooth surface as the comparison tooth surface, analysis of the influence of the modification factor on the error of the left and right flanks. Figure 18a is the cloud diagram of the error distribution of the left and right tooth surfaces corresponding to the situation of no modification. It can be seen from the figure that the maximum error of the left and right tooth surfaces is distributed at the tooth top, in which the maximum error of the left tooth surface is 25 μm and the maximum error of the right tooth surface is 23 μm. Figure 18b is the cloud diagram of tooth surface error corresponding to different modification coefficients. The modification coefficient of the left tooth surface is 0.0005, and the maximum error is about 14 μm. The modification coefficient of the right tooth surface is 0.0004 and the maximum error is about 15 μm.

Figure 19 is error topological diagrams corresponding to different correction coefficients of left and right tooth surfaces. It can be seen from the figure that the tooth surface obtained according to the parabola modification edge envelope can significantly reduce the tooth surface error.

6 Conclusion

1. This paper proposed a new type of skiving method for face gear. According to the principle of gear generating machining, continuously adjust the offset distance between the rotary axis of the skiving tool and the rotary axis of the face gear to be machined, and make the skiving tool feed along the tooth direction so that the gear skiving tool can efficiently cut the design tooth profile on the face

gear to be machined, which can effectively improve the machining efficiency and accuracy of face gear.

2. Based on the principle of the skiving and generating motion, the calculation method of the cutting edge of skiving tool and a method of solving the tooth surface of face gear based on the contour envelope of the discrete cutting edge is proposed. The conjugate surface of the gear skiving tool is solved according to the tooth profile of the modified rack cutter. The intersection of the rake face and the conjugate surface is solved by Newton iterative method. The mathematical model of the gear skiving tool is constructed by importing the cutting edge data to the CAD software, and the envelope profile of the cutting edge is extracted to obtain the gear tooth surface model.
3. This paper analyzed the error source of the face gear skiving machining and proposed a modification method for the skiving tool. The model of the skiving tool is deduced with a bilateral parabola modified rack tool and analyzed the tool tooth profile and the machining tooth surface error. The result shows that when the modification coefficient a are 0.0005 and 0.0004, respectively, the error of left and right tooth profiles are generally low. Compared with the gear without profile modification, the tooth surface error is reduced by 11 and 8 μm, respectively.

Author contribution Shuai Mo proposed the detailed method and theoretical analysis. Saisai Wang proposed the research idea and technical scheme. Bingrui Luo carried out the formula derivation and part of data analysis. Shuai Mo was responsible for completing the article. Heyun Bao, Guojian Cen, and Yunsheng Huang were involved in the discussion and significantly contributed to making the final draft of the article. All the authors read and approved the final manuscript.

Funding This research is financially supported by the National Key Laboratory of Science and Technology on Helicopter Transmission (no. HTL-0-21G07), the Interdisciplinary Scientific Research Foundation of GuangXi University (no.2022JCC022), the Open Fund of State Key Laboratory of Digital Manufacturing Equipment and Technology, the Huazhong University of Science and Technology (no. DMETKF2021017), the National Natural Science Foundation of China (no. 51805368), the Young Elite Scientists Sponsorship Program by CAST (no. 2018QNRC001), and the Entrepreneurship and Innovation Talent Program of Taizhou City, Jiangsu Province.

Data availability The authors confirm that the data supporting the findings of this study are available within the article.

Code availability Not applicable.

Declarations

Ethics approval Not applicable.

Consent to participate Not applicable.

Competing interests The authors declare no competing interests.

References

1. Litvin FL, Fuentes A, Zanzi C, Pontiggia M (2002) Design, generation, and stress analysis of two versions of geometry of face-gear drives. Mech Mach Theory 37:1179–1211. https://doi.org/10.1016/S0094-114X(02)00050-2
2. Zschippang HA, Weikert S, Küük KA, Wegenerb K (2019) Face-gear drive: geometry generation and tooth contact analysis. Mech Mach Theory 142:1–37. https://doi.org/10.1016/j.mechmachtheory.2019.103576
3. Tang JY, Yin F, Chen XM (2013) The principle of profile modified face-gear grinding based on disk wheel. Mech Mach Theory 70:1–15. https://doi.org/10.1016/j.mechmachtheory.2013.06.013
4. He GQ, Zhang SY, Wu TP, Zhao N (2021) An approximate design method of grinding worm with variable meshing angle and grinding experiments of face gear. Mech Mach Theory 166:104461. https://doi.org/10.1016/j.mechmachtheory.2021.104461
5. Wang Y, Tang W, Yin Y, Lan Z, Hou L, Jia S (2017) Hobbing method of face gear based on spherical hob. J Beijing Univ Aeronaut Astronaut 43:441–448. https://doi.org/10.13700/j.bh.1001-5965.2016.0826
6. Zhou YS, Wu YH, Wang LM, Tang JY, Ouyang H (2019) A new closed-form calculation of envelope surface for modeling face gears. Mech Mach Theory 137:211–226. https://doi.org/10.1016/j.mechmachtheory.2019.03.024
7. Mo S, Yue ZX, Feng ZY, Shi LJ, Zhou ZX, Dang HY (2020) Analytical investigation on load-sharing characteristics for multi-power face gear split flow system. Proc Inst Mech Eng C J Mech Eng Sci 234:676–692. https://doi.org/10.1177/0954406219876954
8. Mo S, Zhang T, Jin GG, Cao XL, Gao HJ (2020) Analytical investigation on load sharing characteristics of herringbone planetary gear train with flexible support and floating sun gear. Mech Mach Theory 234(2):1–27. https://doi.org/10.1016/j.mechmachtheory.2019.103670
9. Mo S, Song YL, Feng ZY, Song WH, Hou MX (2021) Research on dynamic load sharing characteristics of double input face gear split-parallel transmission system. J Mech Eng Sci 236:2185–2202. https://doi.org/10.1177/09544062211026349
10. Mo S, Zhou CP, Dang HY (2022) Lubrication effect of the nozzle layout for arc tooth cylindrical gears. J Tribol 144(3):031202–031214. https://doi.org/10.1115/1.4052680
11. Stadtfeld HJ (2014) Power skiving of cylindrical gears on different machine platforms. Gear technology 31:52–62
12. Tapoglou N (2019) Calculation of non-deformed chip and gear geometry in power skiving using a CAD-based simulation. Int J Adv Manufact Technol 100:1779–1785. https://doi.org/10.1007/s00170-018-2790-3
13. Li J, Lou BC, Chen XC (2014) Structural design of slice cutter based on free-form surface. Journal of Mechanical Engineering 50:158–164. https://doi.org/10.3901/JME.2014.17.157
14. Chen XC, Li J, Lou BC (2013) A study on the design of error-free spur slice cutter. Int J Adv Manufact Technol 68:727–738. https://doi.org/10.1007/s00170-013-4794-3
15. Guo Z, Mao SM, Liang HY, Duan DS (2018) Research and improvement of the cutting performance of skiving tool. Mech Mach Theory 120:302–313. https://doi.org/10.1016/j.mechmachtheory.2017.08.004
16. Jia K, Guo J, Ma T, Shaoke W (2021) Mathematical modelling of power skiving for general profile based on numerical enveloping. Int J Adv Manufact Technol 116:733–746. https://doi.org/10.1007/s00170-021-07485-6
17. Su JZ, Wang YQ, Wang P (2021) Modification design and optimization of skiving tool for internal gear. Journal of Xi'an Jiaotong University (Science and Technology) 55:1–6

18. Uriu K, Osafune T, Murakami T, Nakamura M, Iba D, Funamoto M, Moriwaki I (2017) Effects of shaft angle on cutting tool parameters in internal gear skiving. J Mech Sci Technol 31:5665–5673. https://doi.org/10.1007/s12206-017-1107-z
19. He S, Xuan JP, Du WH (2020) Spiral tool path generation method in a NURBS parameter space for the ultra-precision diamond turning of freeform surfaces. J Manuf Process 60:340–355. https://doi.org/10.1016/j.jmapro.2020.10.073
20. Guo EK, Hong RJ, Huang XD, Fang C (2016) Sci Technol 47:70–76. https://doi.org/10.11817/j.issn.1672-7207.2016.01.011
21. Wu ZY, Wang SM, Zhao DX (2019) Analyses on internal gear skiving accuracy influence by shaft angle error. China Mechanical Engineering 30:2412–2423. https://doi.org/10.3969/j.issn.1004-132X.2019.20.003